Adsorption (2014) 20:565–575
DOI 10.1007/s10450-014-9601-4

Sorption of trifluoromethane in activated carbon

**Mark B. Shiflett · David R. Corbin ·
Beth A. Elliott · Shekhar Subramoney ·
Katsumi Kaneko · Akimichi Yokozeki**

Received: 8 September 2013 / Accepted: 8 January 2014

Abstract Sorption isotherms for trifluoromethane (R-23) in activated carbon have been measured at ca. 298 and 323 K using a gravimetric microbalance. High-resolution TEM images of the activated carbon show a very uniform microstructure with no evidence of any contaminants. The adsorption in the activated carbon reaches about 22.8 mol kg^{-1} at 2.0 MPa and 298 K or 17.6 mol kg^{-1} at 2.0 MPa and 323 K. Three different adsorption models (Langmuir, multi-site Langmuir, and BET equations) have been used to analyze the activated carbon sorption data, with a particular interest in the heat of adsorption ($-\Delta H$). The heat of adsorption for R-23 in the activated carbon was about 29.78 ± 0.04 kJ mol^{-1} based on the multi-site Langmuir model and is within the range of typical physical adsorption. According to the IUPAC classification, the activated carbon exhibits Type I adsorption behavior and was completely reversible. Compared with our previous work for the sorption of R-23 in zeolites (5A (Ca,Na-A), 13X (Na-X), Na,K-LSX, Na-Y, K,H-Y, Rb,Na-Y) and ionic liquids ([omim][TFES] and [emim][Tf$_2$N]) the activated carbon had the highest adsorption capacity. The adsorption process in the activated carbon also took less time than in the zeolites or the ionic liquids to reach thermodynamic equilibrium.

Keywords Gas solubility · Activated carbon · Trifluoromethane · Heat of adsorption

1 Introduction

Trifluoromethane (CHF_3, R-23) is an unwanted by-product from the production of chlorodifluoromethane ($CHClF_2$, R-22) due to its high global-warming potential. R-22 is used as a refrigerant in air-conditioning applications and as a feedstock for the production of tetrafluoroethylene ($F_2C{=}CF_2$, TFE); however, R-23 has only limited use as a refrigerant in low-temperature applications. In our original work (Shiflett et al. 2013a, b), we studied six zeolites [5A (Ca,Na-A), 13X (Na-X), Na,K-LSX, Na-Y, K,H-Y, and Rb,Na-Y] and two ionic liquids ([omim][TFES] and [emim][Tf$_2$N]) to capture R-23 from a vent stream. In the present work, we study the adsorption behavior of R-23 in activated carbon at about 298 and 323 K from 0.001 to 2 MPa. To the best of our knowledge, such work has never been reported in the literature. Activated carbon is a form of micro-porous carbon with typically high surface area and pore volume (Yang 2003). We believe that activated carbons, zeolites and ionic liquids have the potential of providing precise and specific separation of gases such as the removal of fluorocarbons from air and nitrogen waste streams.

Olah and coworkers at the University of Southern California have figured out how to use R-23 as a fluorinating agent (Surya Prakash et al. 2012). They found that using the base potassium hexamethyldisilazide in tetrahydrofuran solvent will activate the C–H bond in R-23 (CHF_3). Several reactions to other intermediates have been proposed such as adding elemental sulfur to R-23 to produce trifluoromethanesulfonic acid (CF_3SO_3H). This work may make it

---

M. B. Shiflett (✉) · D. R. Corbin · B. A. Elliott ·
S. Subramoney
DuPont Central Research and Development, Experimental
Station, Wilmington, DE 19880, USA
e-mail: mark.b.shiflett@usa.dupont.com

K. Kaneko
Research Center for Exotic NanoCarbons, Shinshu University,
Nagano, Japan

A. Yokozeki
32 Kingsford Lane, Spencerport, New York, NY 14559, USA

possible to utilize the R-23 by-product captured from the R-22 process.

The present adsorption data of R-23 in activated carbon has been analyzed using three adsorption models with a particular interest in calculating the heat of adsorption: (1) Langmuir (Moore 1972) (2) multi-site Langmuir (Nitta et al. 1984; Bhatia and Ding 2001), and (3) BET (Brunauer et al. 1938) equations. These models have also been used successfully to correlate the adsorption of R-23 in zeolites (Shiflett et al. 2013a, b). In addition, we have correlated the solubility (VLE: vapor–liquid equilibria) of R-23 in ionic liquids [omim][TFES] and [emim][Tf_2N] with our generic Redlich–Kwong (RK) equation of state (EOS) model (Shiflett et al. 2013a, b; Shiflett and Yokozeki 2013). The present adsorption data in activated carbon is compared with our previous work in zeolites and ionic liquids and R-23 molality versus pressure comparisons are discussed.

2 Experimental

2.1 Materials

Trifluoromethane (R-23, CHF_3, purity >99.995 %, molecular weight 70.014 g mol^{-1}, CAS no. 75-46-7) was purchased from GTS-Welco (Allentown, PA, USA). The activated carbon was synthesized from coal tar pitch. The pitch was stabilized by heating to 573 K. The carbon was activated by heating to about 1,153–1,173 K in the presence of potassium hydroxide (KOH) vapors. In order to dry the carbon and remove any residual KOH vapor or adsorbed gases from the pores, the activated carbon was heated in a vertical tube furnace at 623 K for 24 h under vacuum. The surface area and pore volume were measured by nitrogen adsorption/desorption measurements, performed at 77 K on a Micromeritics ASAP model 2420 porosimeter. Samples were degassed at 423 K overnight prior to data collection. Surface area measurements utilized a five-point adsorption isotherm collected over 0.05–0.20 P/P_0 (P_0 = nitrogen saturation pressure) and analyzed via the BET method (Brunauer et al. 1938). Total pore volume was determined by a single point measurement at $P/P_0 = 0.995$. The BET specific surface area was 3,206 $m^2\ g^{-1}$ with a type I isotherm. The BET model has inaccuracies for micropore systems which can lead to condensation even at low relative pressure and, correspondingly, to an overestimation of the surface area (Kaneko et al. 1992). The BET specific surface area is a reproducible measurement, characteristic of the material, but possibly an overestimation of the total surface area. The total pore volume is 1.68 $cm^3\ g^{-1}$ with an average pore diameter of 2.0 nm.

2.2 Microscopy

The microstructure of the activated carbon was analyzed by high-resolution transmission electron microscopy (TEM) and its associated elemental analysis by energy dispersive spectroscopy (EDS) using a Tecnai F-20 scanning transmission electron microscope (STEM) equipped with a field-emitting electron source. The microscope was operated at an accelerating voltage of 200 kV. The elemental analysis was accomplished with an Oxford Instruments INCA x-sight EDS system attached to the microscope column and capable of identifying elements as light as boron. This particular EDS system has a Li-doped Si detector and an ATW ultra-thin window. The activated carbon sample was dispersed onto holey-carbon coated copper TEM grids by dry dusting.

2.3 Vapor–liquid equilibria and adsorption measurements using a gravimetric microbalance

A gravimetric microbalance is a common method used to measure the solubility of gases in sorbents. The method was originally developed to accurately measure the gas adsorption in solids (e.g., zeolites); however, it can also be used to measure the gas absorption in ionic liquids due to their low vapor pressure. We have extensively used a Hiden gravimetric microbalance (IGA003) (Hiden Isochema, Ltd., Warrington, United Kingdom, www.hidenisochema.com) to measure the solubility and diffusivity of many different gases [CO_2, SO_2, hydrofluorocarbons (HFCs) and hydrofluoroethers (HFEs)] in ionic liquids over a range of temperatures (283–348 K) and pressures (0–2 MPa) (Shiflett et al. 2006a, b, 2012a, b; Shiflett and Yokozeki 2006a, 2007a, b, c, 2008, 2009a, b, 2010, 2011). The advantages of using a microbalance include the minimal sample size (<100 mg) required, the ability to automate the measurement process to take several *PTx* data, and the flexibility to measure both absorption and desorption isotherms. When done properly, the gravimetric analysis provides a direct and accurate method for assessing both gas solubility and diffusivity (Shiflett and Yokozeki 2005). Two critical factors that must be considered include properly correcting for the buoyancy effects of the system and allowing sufficient time to reach equilibrium (i.e., no mixing is possible) (Shiflett and Yokozeki 2006a, b). In particular, the sorption of gases in activated carbons, zeolites and ionic liquids is a diffusion-controlled gas sorption process which can take several hours or days to reach equilibrium at a given *T* and *P*. A detailed description of the microbalance equipment and procedures are available in our previous reports (Shiflett and Yokozeki 2005, 2006b). The critical details for properly correcting for a number of balance forces are provided in the following references (Shiflett and Yokozeki 2005, 2006b; Shiflett et al. 2012a). Only the basic experimental techniques and measurement uncertainties are given here.

The adsorption and desorption measurements were performed in static mode in this study. The sample temperature was measured with a resistance temperature device (RTD) with an accuracy of ±0.1 K. The RTD was calibrated using a standard platinum resistance thermometer (SPRT model 5699, Hart Scientific, American Fork, UT, range 73–933 K) and readout (Blackstack model 1560 with SPRT module 2560). The Blackstack instrument and SPRT are a certified secondary temperature standard with a NIST traceable accuracy to ±0.005 K. Two isotherms of about 298–323 K were measured beginning with 298 K. Two pressure sensors were used for the measurements. Pressures from 10^{-4} to 10^{-2} MPa were measured using a capacitance manometer (MKS, model Baratron® 626A) with an accuracy of ±0.015 kPa. Pressures from 10^{-2} to 2.0 MPa were measured using a piezo-resistive strain gauge (Druck, model PDCR4010) with an accuracy of ±0.8 kPa. The Druck low-pressure transducer was calibrated against a Paroscientific Model 765-15A (Redmond, WA, USA) pressure transducer (range 0–0.102 MPa, Part no. 1100-001, Serial no. 104647). The Druck high-pressure transducer was calibrated against a Paroscientific Model 765-1 K (Redmond, WA, USA) pressure transducer (range 0–6.805 MPa, Part no. 1100-017, Serial no. 101314). The calibration pressure transducers are also NIST-certified secondary pressure standards with a traceable accuracy of 0.008 % of full scale. The upper pressure limit of the microbalance reactor was 2.0 MPa. Several isobars up to 2.0 MPa (0.001, 0.002, 0.003, 0.004, 0.005, 0.006, 0.007, 0.008, 0.009, 0.01, 0.025, 0.05, 0.1, 0.25, 0.50, 0.75, 1.00, 1.25, 1.50, 1.75, 2.00 MPa) were measured for R-23 in activated carbon. In our previous work with zeolites (Shiflett et al. 2013a, b) to ensure sufficient time for VLE, each T,P condition was maintained for a minimum of 10 h with a maximum time of 20 h. In this work, we set the same minimum and maximum time for isotherms measured at 298–323 K. The total uncertainties in the solubility data due to both random and systematic errors have been estimated to be less than 0.006 mol fraction at given T and P. The equivalent uncertainty in molality for activated carbon is 0.5 mol kg^{-1} at given T and P. The corrected solubility (*PTx*) data for R-23 in the activated carbon is shown in Tables 1 and 3. Desorption isotherms were also measured at 298–323 K and the (*PTx*) data are included in Tables 2 and 4. The R-23 mass uptake between 0 and 2.0 MPa at 298 and 323 K indicate the sorption is reversible.

Table 1 Experimental adsorption measurements for R-23 (1) in activated carbon (2) at 298.1 K

T (K)	P (MPa)	wt%	100 x_1	Molality (mol kg^{-1})
298.1	0.0010	0.76	0.0013	0.109
298.1	0.0020	1.39	0.0024	0.201
298.1	0.0030	1.96	0.0034	0.286
298.1	0.0040	2.45	0.0043	0.359
298.1	0.0050	2.93	0.0051	0.431
298.1	0.0060	3.36	0.0059	0.497
298.1	0.0070	3.76	0.0067	0.558
298.1	0.0080	4.16	0.0074	0.620
298.1	0.0090	4.55	0.0081	0.681
298.1	0.0102	4.88	0.0087	0.733
298.1	0.0248	9.22	0.0171	1.451
298.1	0.0498	14.54	0.0283	2.430
298.1	0.0996	21.90	0.0459	4.005
298.1	0.2438	34.06	0.0814	7.378
298.1	0.4531	42.87	0.1140	10.72
298.1	0.7492	49.54	0.1442	14.02
298.1	0.9972	53.10	0.1626	16.17
298.1	1.2489	55.86	0.1784	18.08
298.1	1.4992	58.06	0.1919	19.77
298.1	1.7494	59.90	0.2039	21.34
298.1	1.9989	61.45	0.2147	22.77

Table 2 Experimental desorption measurements for R-23 (1) in activated carbon (2) at 298.1 K

T (K)	P (MPa)	wt%	100 x_1	Molality (mol kg^{-1})
298.1	1.9963	61.47	0.2148	22.79
298.1	1.7476	59.91	0.2040	21.34
298.2	0.4431	42.60	0.1129	10.60
298.1	0.2499	34.49	0.0828	7.520
298.1	0.0998	21.98	0.0461	4.024
298.1	0.0748	18.64	0.0378	3.272
298.1	0.0499	14.57	0.0284	2.436
298.1	0.0249	9.30	0.0173	1.465
298.1	0.0099	4.86	0.0087	0.730
298.1	0.0093	4.72	0.0084	0.708
298.1	0.0080	4.24	0.0075	0.632
298.1	0.0070	3.85	0.0068	0.572
298.1	0.0060	3.45	0.0061	0.510
298.1	0.0050	3.01	0.0053	0.443
298.1	0.0040	2.53	0.0044	0.371
298.1	0.0030	2.03	0.0035	0.296
298.1	0.0020	1.47	0.0026	0.213
298.1	0.0010	0.84	0.0015	0.121

Table 3 Experimental adsorption measurements for R-23 (1) in activated carbon (2) at 323.1 K

T (K)	P (MPa)	wt%	100 x_1	Molality (mol kg^{-1})
323.2	0.0010	0.23	0.0004	0.033
323.1	0.0020	0.55	0.0010	0.079
323.1	0.0030	0.85	0.0015	0.122
323.2	0.0040	1.14	0.0020	0.165
323.2	0.0050	1.40	0.0024	0.203
323.1	0.0060	1.65	0.0029	0.240
323.2	0.0070	1.90	0.0033	0.277
323.1	0.0080	2.15	0.0038	0.314
323.1	0.0090	2.38	0.0042	0.348
323.2	0.0099	2.53	0.0044	0.371
323.2	0.0248	5.37	0.0096	0.811
323.2	0.0498	9.05	0.0168	1.421
323.1	0.0746	12.00	0.0229	1.948
323.2	0.0999	14.63	0.0286	2.448
323.1	0.2488	25.37	0.0551	4.855
323.1	0.4977	35.54	0.0864	7.875
323.2	0.7493	41.63	0.1090	10.19
323.1	0.9995	45.77	0.1265	12.06
323.3	1.2428	48.80	0.1405	13.61
323.1	1.4988	51.36	0.1534	15.08
323.1	1.7492	53.41	0.1643	16.37
323.0	1.9927	55.13	0.1741	17.55

Table 4 Experimental desorption measurements for R-23 (1) in activated carbon (2) at 323.1 K

T (K)	P (MPa)	wt%	100 x_1	Molality (mol kg^{-1})
323.2	1.9912	55.13	0.1741	17.55
323.2	1.7384	53.37	0.1641	16.35
323.2	1.4931	51.34	0.1532	15.07
323.1	1.2496	48.88	0.1409	13.66
323.2	0.9997	45.78	0.1265	12.06
323.2	0.7457	41.57	0.1088	10.16
323.1	0.4995	35.63	0.0867	7.906
323.2	0.2499	25.50	0.0555	4.889
323.2	0.0999	14.66	0.0286	2.454
323.1	0.0749	12.12	0.0231	1.970
323.1	0.0498	9.11	0.0169	1.432
323.1	0.0249	5.45	0.0098	0.823
323.1	0.0099	2.58	0.0045	0.378
323.2	0.0090	2.43	0.0042	0.356
323.2	0.0080	2.21	0.0039	0.323
323.2	0.0070	1.98	0.0035	0.289
323.1	0.0060	1.72	0.0030	0.250
323.1	0.0050	1.48	0.0026	0.215
323.2	0.0040	1.21	0.0021	0.175
323.1	0.0030	0.93	0.0016	0.134
323.1	0.0020	0.63	0.0011	0.091
323.2	0.0010	0.31	0.0005	0.044

3 Analyses and results

Ultra-thin fragments of the carbon suspended over the holes were analyzed by imaging and EDS for elemental composition. Figure 1 shows conventional bright-field and high-resolution TEM images of the activated carbon showing a very uniform microstructure with no evidence of any contaminants. The high-resolution image clearly demonstrates that the (0002) basal planes of the carbon comprising the activated carbon show little to no preponderance to stack by van der Waals forces, a key parameter contributing to the ultra-high surface area of this carbon. Figure 2 shows a high-angle annular dark-field (HAADF) STEM image of the carbon along with an accompanying EDS spectrum from the area outlined by the box. The HAADF image as well as the EDS spectrum clearly demonstrates that no contaminants are detectable other than oxygen, likely from exposure of the carbon to ambient air.

The experimental data for R-23 adsorption isotherms in activated carbon zeolites has been analyzed using the same theoretical models as in our previous work (Shiflett et al. 2013a, b): (1) Langmuir equation (Surya Prakash et al. 2012), (2) multi-site Langmuir equation (Nitta et al. 1984; Bhatia and Ding 2001), and (3) BET equation (Brunauer et al. 1938). In order to compare the adsorption capacity with the solubility capacity in an ionic liquid, solubility data of binary mixtures of R-23 and ionic liquids ([omim][TFES] and [emim][Tf$_2$N]) have been analyzed using a modified Redlich–Kwong (RK) EOS (Shiflett and Yokozeki 2013). A brief description of each model is provided and additional details can be found in our previous work (Shiflett et al. 2013a; b).

3.1 Langmuir model

The Langmuir adsorption isotherm is simply derived from a kinetic mechanism of the condensation and evaporation of gas molecules at the surface (Moore 1972). The adsorption process between gas phase molecules (A), vacant surface sites (S), and occupied surface sites (AS) can be represented by the "reaction" equation,

$$A + S = AS, \tag{1}$$

assuming that there are a fixed number of surface sites present on the surface. Then, an equilibrium constant, K, can be written:

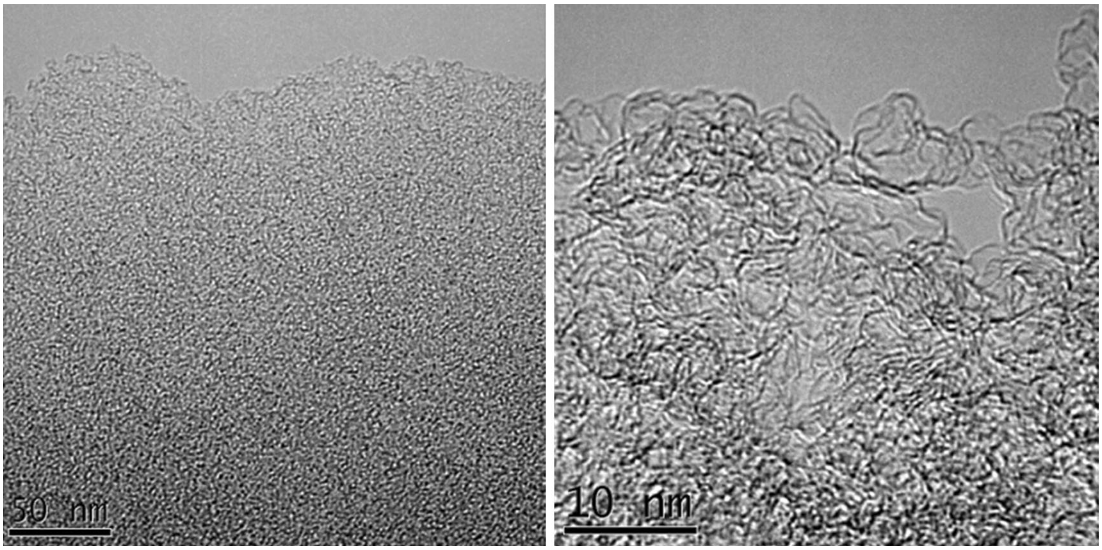

Fig. 1 Conventional TEM bright-field (*left*) and ultra-high-resolution (*right*) TEM images of the activated carbon

Fig. 2 HAADF image and corresponding EDS analysis of the activated carbon showing the presence of no contaminants other than oxygen, likely from exposure to ambient air

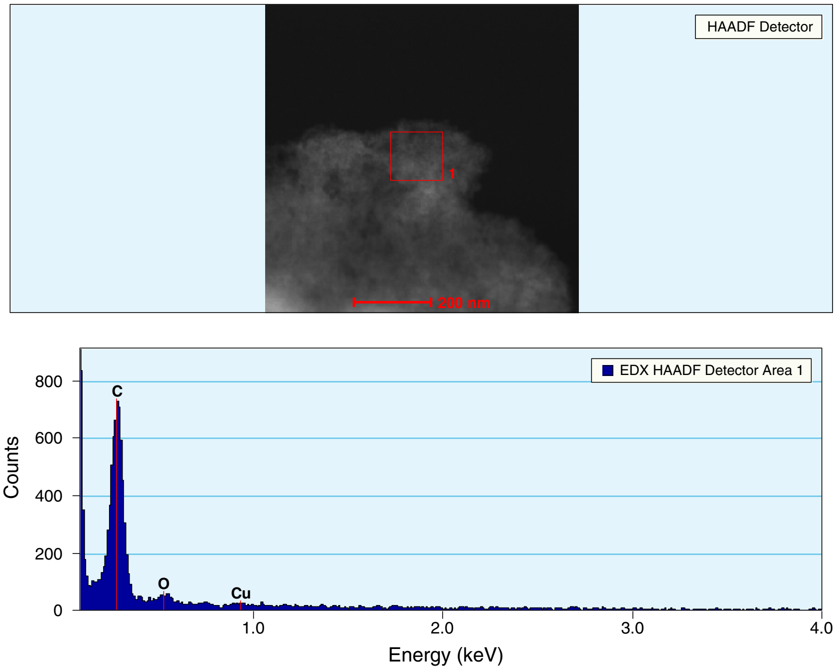

$$K = \frac{k_a}{k_d} = \frac{[AS]}{[S][A]}, \tag{2}$$

where k_a and k_d are adsorption and desorption rate constants. When we introduce a fraction (θ) of surface sites occupied ($0 \leq \theta \leq 1$), $[AS]$ is proportional to θ, $[S]$ is proportional to $(1-\theta)$, and $[A]$ is proportional to the pressure of gas, P. Thus, it is possible to define a new equilibrium constant, b for K:

$$b \equiv \frac{\theta}{(1-\theta)P} \propto K, \tag{3}$$

By rearranging this equation, we have the expression for surface coverage for the Langmuir adsorption equation:

$$\theta = \frac{bP}{1+bP} = \frac{P}{1/b+P}. \tag{4}$$

Using a thermodynamic relation between Gibbs free energy ΔG and an equilibrium constant K, ($\Delta G = \Delta H - T\Delta S = -RT\ln K$), the parameter, b in Eqs. (3) and (4), can be written as,

$$b = b_0 e^{-\Delta H/RT} \equiv b_0 e^{\varepsilon_0/RT}, \tag{5}$$

where R is the gas constant, and b_0 contains a proportionality constant in Eq. (3) and ΔS (entropic change term). As a working equation, Eq. (4) is not convenient, since a direct experimental quantity for adsorption is not the coverage fraction, θ, but is an amount of adsorbed molecules (absorbates) in a given adsorbent; often conveniently expressed as molality, q (mol kg^{-1}), as shown in Tables 1, 2, 3, 4. When a maximum coverage of sites (or monolayer of adsorption) is written as c (mol kg^{-1}), the coverage fraction is given by $\theta = q/c$. Therefore, a working equation for Eq. (4) becomes:

$$q = \frac{cP}{1/b + P} = \frac{cP}{k_0 e^{-\varepsilon_0/RT} + P}, \tag{6}$$

where k_0 (= $1/b_0$) has the same unit as pressure.

Experimental data for the R-23 adsorption isotherms (298.15–323.15 K) in activated carbon have been analyzed using Eq. (6). Three unknown parameters, c, k_0, and ΔH (or $= \varepsilon_0$) have been determined by the use of a non-linear least square regression method: the object function = sum of (T, P) data of $[q(\text{observed}) - q(\text{calculated})]^2$. Using this fitting process, it was found that not all the data can be fitted, particularly for the data measured at higher pressures. This fact is understandable since the Langmuir equation is based on the assumption that adsorption is limited up to a monolayer coverage (often only good for "infinite dilution" or *Henry's law* region). Further gas adsorptions at higher pressures are not valid for this equation. Valid regions for the equation were found by a trial-and-error method; eliminating high pressure data step by step to see whether the physical condition, θ (= q/c) < 1, is satisfied. Determined parameters are listed in Table 5; for activated carbon, $P < 0.006$ MPa and AAD (Absolute average deviation = $\{1 - \text{q(observed)/q(calculated)}\} \times 100/\text{number of data}$) = 3.63 %. If all experimental data are used, $P < 2.0$ MPa and the AAD = 30.9 %. Fitted equations are compared with experimental data as θ (= q/c) in Figs. 3 and 4.

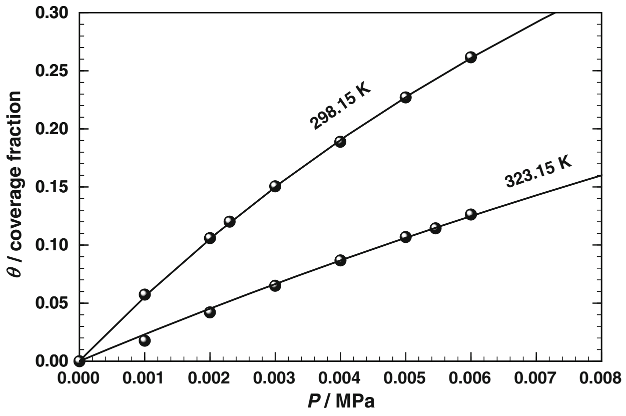

Fig. 3 R-23 adsorption isotherms in activated carbon: coverage fraction $\theta = q/c$ versus pressure (<0.006 MPa). *Solid circles* experimental data. *Solid lines* calculated using the original Langmuir model Eq. (6) with parameters in Table 5

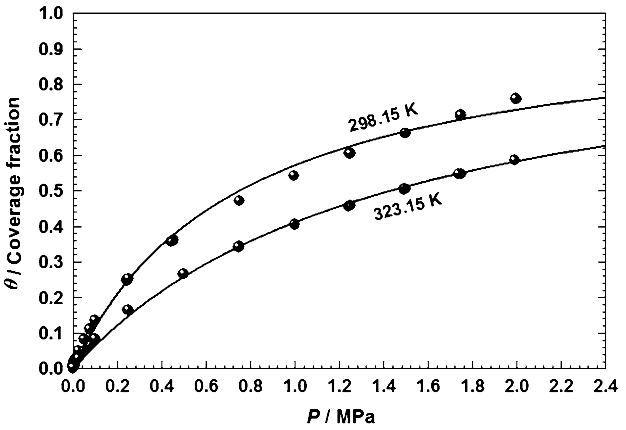

Fig. 4 R-23 adsorption isotherms in activated carbon: coverage fraction $\theta = q/c$ versus pressure (<2.0 MPa). *Solid circles* experimental data. *Solid lines* calculated using the original Langmuir model Eq. (6) with parameters in Table 5

3.2 Multi-site Langmuir model

In order to improve the Langmuir model, Nitta et al. developed a statistical mechanical model using a concept of "multi-site occupancy" adsorptions, in which a molecule occupies both single- and multi-site adsorptions, and also it includes a molecular interaction parameter for adsorbate–adsorbate interactions (Nitta et al. 1984). Later, this model was justified by classical thermodynamic equations by Bhatia and Ding (2001). For a general n multi-component ($i = 1,\ldots,n$) adsorption system with σ_i, which is the number of sites occupied by one molecule, it is given by, neglecting adsorbate–adsorbate interactions;

$$\theta_i = \sigma_i K_i P_i \left(1 - \sum_{j=1}^{n} \theta_j\right)^{\sigma_i}. \tag{7}$$

Table 5 Non-linear least-squares analysis of R-23 adsorption data for Eq. (6)

	c (mol kg^{-1})	k_0 (bar)	ε_0 (kJ mol^{-1})	p (MPa)
Activated carbon	1.8964 ± 0.1367	$2.056 \times 10^4 \pm 3.345 \times 10^3$	−29.01 ± 0.51	<0.006
Activated carbon	29.716 ± 0.470	$3.275 \times 10^4 \pm 8.484 \times 10^3$	−20.78 ± 0.69	<2.0

This equation may be reduced to the following working equation for $n = 1$ (Cavenati et al. 2004):

$$q = cf(T)P(1 - q/c)^{\sigma}, \tag{8}$$

where

$$f(T) = k_m \exp(-\varepsilon_m/RT), \tag{9}$$

and c is the same quantity as that in Eq. (6). Cavenati et al. successfully applied Eq. (8) for N_2, CH_4, and CO_2 adsorptions in zeolite 13X in a wide range of pressures (from 0 to 50 bar at $T = 298$, 308, and 323 K) (Cavenati et al. 2004).

The present adsorption data were also analyzed with Eq. (8). Now we have four adjustable parameters: c, k_m, ε_m, and σ. These parameters have been determined by a non-linear least-square regression with an object function of a sum of $\{\ln[q(\text{calculated})/q(\text{observed})] - 1\}^2$; here q in Eq. (8) is an implicit function that must be solved numerically first. The analysis showed that the present isotherm data for the entire pressure region (up to 2.0 MPa) could not be fitted well, although the valid region of fittings increased relative to the original Langmuir Eq. (6). The proper fitting region was found in a way similar to the case of Eq. (6). Determined parameters are listed in Table 6; for activated carbon, $P < 0.01$ MPa and AAD = 3.31 %. Fitted equations are compared with experimental data as θ (=q/c) in Fig. 5.

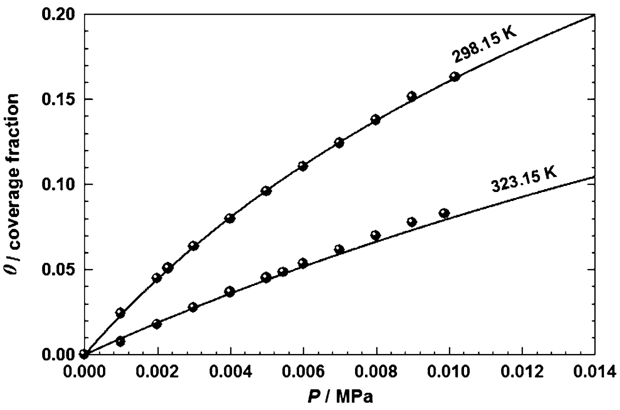

Fig. 5 R-23 adsorption isotherms in activated carbon: coverage fraction $\theta = q/c$ versus pressure (<0.011 MPa). *Solid circles* experimental data. *Solid lines* calculated using the multi-site Langmuir model Eq. (8) with parameters in Table 6

3.3 BET model

Molecules can also often form multilayers, that is, some are adsorbed on already adsorbed molecules and the Langmuir isotherm is not valid. Brunauer, Emmett and Teller (BET) developed a model isotherm that takes that possibility into account (Brunauer et al. 1938). They extended the Langmuir "reaction" mechanism, Eq. (1) as:

$$A + S = AS$$

$$A + AS = A_2S$$

$$A + A_2S = A_3S, \quad \text{and} \quad \text{so on.}$$

This infinite series of reactions can be analytically solved and written in the following BET equation:

$$\frac{1}{v[(P_0/P) - 1]} = \frac{s-1}{v_m s}\left(\frac{P_0}{P}\right) + \frac{1}{v_h s}, \tag{10}$$

and

$$s \equiv \exp\left(\frac{\varepsilon_1 - \varepsilon_L}{RT}\right), \tag{11}$$

where P and P_0 are the equilibrium and the saturation pressures of adsorbates at the temperature of adsorption respectively, v is the adsorbed gas quantity in volume units at the standard-temperature–pressure (STP) condition, v_m volume (at the STP) is the monolayer adsorbed gas quantity, and ε_1 is the heat of adsorption for the first layer, and ε_L is that for the second and all higher layers. A major application of this model is often used in surface science to characterize the specific surface area of an absorbing solid. For example, Eq. (10) can be plotted as a straight line with $1/v$ $[(P_0/P) - 1]$ on the y-axis and P/P_0 on the x-axis according to experimental results (i.e., BET plot). The linear relationship of this equation is known to be maintained only in the range of $0.05 < P/P_0 < 0.35$. The value of the slope and the y-intercept of the line are used to calculate the monolayer adsorbed gas quantity v_m and the BET constant s. However, one of the problems of Eq. (10) is the limitation of experimental temperatures: $T < T_c$ (gas critical temperature), since $P_0(T)$ is the vapor pressure of gas. R-23 has $T_c = 299.3$ K, and above this temperature like the present case of 323 K, adsorption isotherms cannot be analyzed by Eq. (10).

Therefore, in the present study, we treat the BET equation as an "effective" (or empirical) fitting equation for adsorption isotherms, assuming that P_0 is an *effective temperature dependent parameter* (not a physical vapor pressure) as well as an *effective T-dependent* v_m. By simple algebraic manipulations, Eq. (10) can be written as:

Table 6 Non-linear least-squares analysis of R-23 adsorption data for Eq. (8)

	c (mol kg^{-1})	k_m (bar^{-1})	σ	ε_m (kJ mol^{-1})
Activated carbon	4.5000 ± 0.0609	$1.509 \times 10^{-5} \pm 2.45 \times 10^{-7}$	2.515 ± 0.197	−29.78 ± 0.04

Table 7 Non-linear least-squares analysis of R-23 adsorption data for Eq. (12)

	T (K)	α (bar^{-1})	β (bar^{-2})	γ (bar^{-1})
Activated carbon	298.15	7.1731 ± 0.260	$-1.002 \times 10^{-2} \pm 2.03 \times 10^{-3}$	0.45959 ± 0.0474
	323.15	3.6338 ± 0.090	$-5.383 \times 10^{-3} \pm 7.42 \times 10^{-4}$	0.26196 ± 0.0161

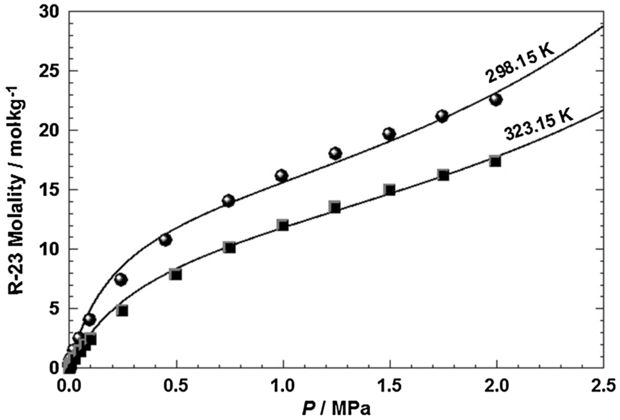

Fig. 6 R-23 adsorption isotherms in activated carbon: adsorption amount (in molality) versus pressure (<2.0 MPa). *Solids circles* experimental data at 298.15 K. *Solid squares* experimental data at 323.15 K. *Solid lines* calculated using the effective BET Eq. (12) with parameters in Table 7

$$q = \frac{\alpha P}{\beta P^2 + \gamma P + 1}, \qquad (12)$$

where $\alpha \equiv csv_m/P_0, \beta \equiv (1-s)/P_0^2$, and$\gamma \equiv (s-2)/P_0$; c is a unit conversion factor from the STP volume v to an adsorbed gas quantity (q: in molality). Here, we have three unknown adjustable parameters, α, β, and γ, which have been determined using a non-linear least-square regression: object function = sum of $[q(\text{observed}) - q(\text{calculated})]^2$ for each isotherm-data set. Optimal parameters using the entire P region data are listed in Table 7 and the calculated data are compared with experimental values in Figs. 6, 7, 8. By considering only three adjustable parameters were used, the data fitting is fairly good for a wide range of experimental pressures (activated carbon at 298–323 K, AAD = 13.57 and 8.262 %). The weak point of this equation is that it cannot fit data sets of different temperatures simultaneously, because of the unknown T dependences on parameters v_m and P_0 (or α, β, and γ). This means that the data correlation is only good for each temperature set, and cannot be used for predicting the other temperature data.

4 Discussion

The adsorption of R-23 in the activated carbon is typically of Type I behavior according to the IUPAC classification and

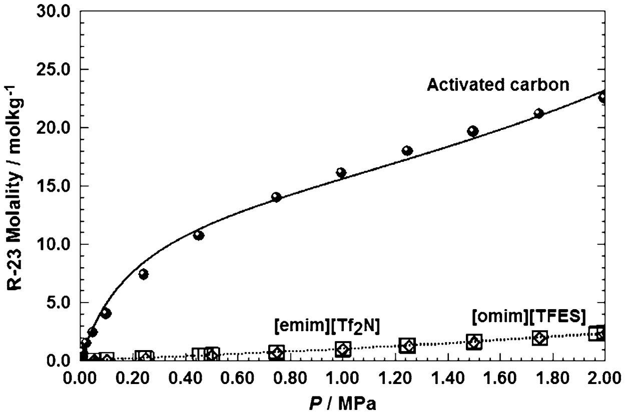

Fig. 7 Comparison of R-23 adsorption isotherms in activated carbon with ionic liquids ([omim][TFES] and [emim][Tf$_2$N]) at 298.15 K: adsorption amount (in molality) versus pressure. Symbols: experimental data, activated carbon, *solid circles*; ionic liquid [omim][TFES], *open diamonds*; ionic liquid [emim][Tf$_2$N], *open squares*. *Solid line* calculated for activated carbon using the effective BET Eq. (12) with parameters in Table 7. *Dashed lines* calculated for ionic liquids using the generic RK EOS with parameters provided in references (Shiflett et al. 2013a, b)

was completely reversible. It is quite interesting to compare the R-23 adsorption in activated carbon with the solubility in ionic liquids and zeolites found in our previous work (Shiflett et al. 2013a, b). The adsorption of R-23 in activated carbon is significantly higher than the solubility of R-23 in ionic liquids ([omim][TFES] and [emim][Tf$_2$N]). Figure 7 shows the adsorption in activated carbon reaches about 22.7 mol kg^{-1} at about 2.0 MPa and 298 K while in the ionic liquid the absorption reaches about 2.37 mol kg^{-1} at about 2.0 MPa and 298 K (Shiflett et al. 2013a). The activated carbon has an order of magnitude greater adsorption compared with the ionic liquid. The adsorption of R-23 in activated carbon is also quite different than the adsorption in zeolites. Figure 8 shows the adsorption of R-23 at low pressures ($P < 0.05$ MPa) in the activated carbon is lower than the adsorption in zeolites [5A (Ca,Na-A), 13X (Na-X), Na,K-LSX] (Shiflett et al. 2013b); however, as the pressure increases ($0.1 < P < 2.0$ MPa) the adsorption in the activated carbon continues to increase while the adsorption in the zeolites remains constant. Figure 9 compares the R-23 coverage fraction in activated carbon with zeolites (Na-Y, K,H-Y, Rb,Na-Y, 5A, 13X and Na,K-LSX) at 298.15 K using the multi-site Langmuir model Eq. (8) with parameters

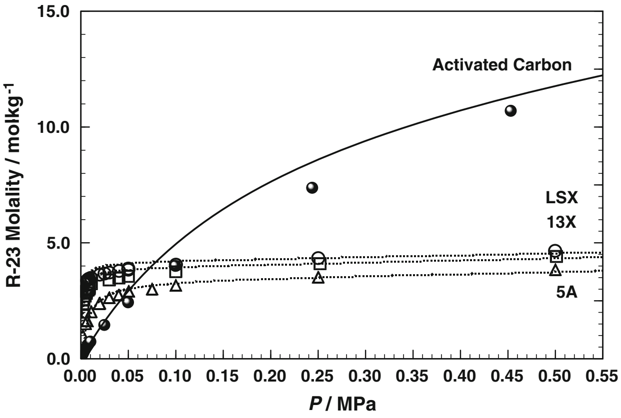

Fig. 8 Comparison of R-23 adsorption isotherms in activated carbon with R-23 solubility in zeolites [5A (Ca,Na-A), 13X (Na-X) and LSX (Na,K-LSX)] at 298.15 K: adsorption amount (in molality) versus pressure. Symbols: experimental data, activated carbon, *solid circles*; zeolite 5A, *open triangles*; zeolite 13X, *open squares*; zeolite LSX, *open circles*. *Solid line* calculated using the effective BET Eq. (12) with parameters in Table 7. *Dashed lines*: calculated for zeolites using the effective BET Eq. (12) with parameters provided in reference (Shiflett et al. 2013b)

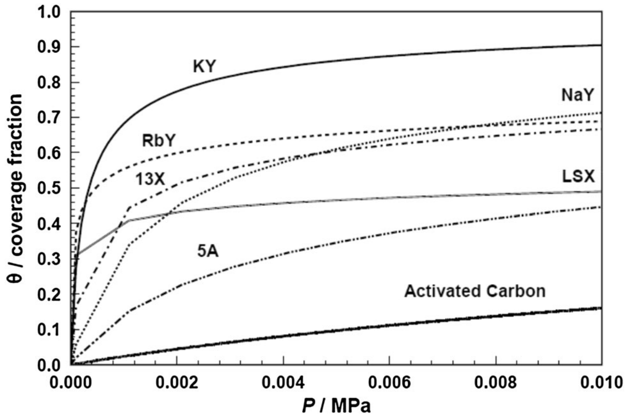

Fig. 9 Comparison of R-23 adsorption isotherms in activated carbon and zeolites [Na-Y, KY (K,H-Y), RbY (Rb,Na-Y), 5A (Ca,Na-A), 13X (Na-X) and LSX (Na,K-LSX)] at 298.15 K; coverage fraction $\theta = q/c$ versus pressure. *Lines* calculated using the multi-site Langmuir model Eq. (8) with parameters in Table 6 and references (Shiflett et al. 2013a, b)

taken from our previous work (Shiflett et al. 2013a). Zeolite K,H-Y had the highest fractional coverage of about 0.85 at 0.0050 MPa. Zeolites Na,K-LSX and 5A had the lowest fractional coverage of about 0.45 and 0.30, respectively at 0.0050 MPa. The activated carbon has the lowest overall fractional coverage at low pressures ($P < 0.010$ MPa) of about 0.23 at 0.0050 MPa. The order from highest to lowest fractional coverage at 0.0050 MPa was K,H-Y > Rb,Na-Y > 13X > Na-Y > Na,K-LSX > 5A > activated carbon.

The heat of adsorption ($-\Delta H$, or $-\varepsilon_0$ and $-\varepsilon_m$) for R-23 in the activated carbon has been estimated using the Langmuir and multi-site Langmuir models to be about 29 ± 0.5 and 29.8 ± 0.04 kJ mol^{-1}, respectively; see Tables 5 and 6 (ε_0 and ε_m). For comparison, the heat of adsorption for R-23 in zeolites Na-Y, K,H-Y and Rb,Na-Y (Shiflett et al. 2013a) has been calculated to be about 35 ± 3, 29 ± 3, and 34 ± 5 kJ mol^{-1}, respectively. These values are similar to the activated carbon and are within a typical physical adsorption range (<50 kJ mol^{-1}) which are similar to those for CO_2 (35.6–37.2 kJ mol^{-1}) adsorption in zeolite 13X (Cavenati et al. 2004; Breck 1974). We have also observed that the adsorption to reach the equilibrium condition with the zeolites takes a much longer time compared with the solubility equilibrium in the activated carbon and the ionic liquids (i.e., hours vs. minutes).

The advantage of using the activated carbon is the adsorption capacity is significantly higher (about 10^1–10^2) than the absorption solubility in the ionic liquids ([omim][TFES], [emim][Tf_2N]) and the zeolites at high pressures ($P > 1.0$ MPa). The sorption for the activated carbon is also completely reversible with a decrease in pressure which is similar to the behavior with the ionic liquids ([emim][Tf_2N] and [omim][TFES]).

The purpose of this work was to identify sorbents which can be used to separate R-23 from an air/nitrogen waste stream. The activated carbon shows promise and provided the highest overall capacity compared with other sorbents studied in our previous works (5A, 13X, Na,K-LSX and [omim][TFES]) [1] and (Na-Y, K,H-Y, Rb,Na-Y and [emim][Tf_2N]) (Shiflett et al. 2013a). However, the best choices may not be based on achieving the highest thermodynamic equilibrium at a given T and P, but rather on the fastest rate of sorption. The R-23 containing waste stream will be passed through either a fixed bed of adsorbent (activated carbon or zeolite) or a column filled with packing and ionic liquid to separate the trifluoromethane from the air/nitrogen. Both the equilibrium and the rate of sorption factor into the size of the bed or column which ultimately determines the cost. Studies are also underway to calculate the rate of diffusion for the activated carbon, zeolites and ionic liquids. Finally, work has also been published using zeolites to purify hexafluoroethane (R-116 or FC-116) containing chlorotrifluoromethane (R-13 or CFC-13) and trifluoromethane (R-23 or HFC-23) which may be of interest to the reader and can be found in reference (Corbin et al. 1996).

5 Conclusions

Adsorption isotherms for R-23 (trifluoromethane) in activated carbon have been measured at 298 and 323 K at pressures up to 2.0 MPa using a gravimetric microbalance.

Classical Type I adsorption behavior according to the IUPAC classification was observed. Three different adsorption models (Langmuir, multi-site Langmuir and BET) have been used to analyze the sorption data with a particular interest in the head of adsorption ($-\Delta H$).

The adsorption of R-23 in activated carbon is significantly higher than the solubility of R-23 in ionic liquids ([omim][TFES] and [emim][Tf_2N]). The R-23 adsorption in activated carbon reaches about 22.7 mol kg^{-1} at about 2.0 MPa and 298 K while in the ionic liquids the absorption reaches about 2.37 mol kg^{-1} at about 2.0 MPa and 298 K. The activated carbon has an order of magnitude higher adsorption capacity relative to the ionic liquids.

The adsorption of R-23 in activated carbon is also quite different than the adsorption in zeolites, particularly at low pressure. The adsorption of R-23 at low pressure ($P < 0.05$ MPa) in the activated carbon is lower than the adsorption in zeolites [5A (Ca,Na-A), 13X (Na-X), Na,K-LSX]; however as the pressure increases ($0.1 < P < 2.0$ MPa) the adsorption in the activated carbon continues to increase while the adsorption in the zeolites remains constant. The R-23 adsorption in zeolites reaches about 5.0–6.0 mol kg^{-1} at about 2.0 MPa and 298 K which is lower than in activated carbon.

Analyses of the present adsorption data of R-23 in activated carbon at 298 and 323 K show the heat of adsorption to be about 29 ± 0.5 and 29.8 ± 0.04 kJ mol^{-1} using the Langmuir and multi-site Langmuir models, respectively. These values are comparable to those measured in previous work for R-23 in zeolites, Na-Y, K,H-Y, Rb,Na-Y, 5A, Na,K-LSX and 13X which were about 35 ± 3, 29 ± 3, and 34 ± 5, 10 ± 3, 30 ± 5, and 40 ± 4 kJ mol^{-1}, respectively.

Acknowledgments The authors thank Dr. Lloyd Abrams (retired), Dr. Alan M. Allgeier and Mr. Brian L. Wells from the DuPont Experimental Station for their assistance with obtaining the surface area and pore volume of the activated carbon and the R-23 gravimetric solubility measurements. The present work was supported by DuPont Central Research and Development.

References

Bhatia, S.K., Ding, L.P.: Vacancy solution theory of adsorption revisited. AIChE J. **47**, 2136–2138 (2001)

Breck, D.W.: Zeolite Molecular Sieves. Wiley, New York (1974)

Brunauer, S., Emmett, P.H., Teller, E.: Adsorption of gases in multimolecular layers. J. Am. Chem. Soc. **60**, 309–319 (1938)

Cavenati, S., Grande, C.A., Rodrigues, A.E.: Adsorption equilibrium of methane, carbon dioxide, and nitrogen on zeolite 13X at high pressures. J. Chem. Eng. Data **49**, 1095–1101 (2004)

Corbin, D.R., Fernandez, R.E., Mahler, B.A.: Purification of Hexafluoroethane Products, US Patent 5,523,499, 4 June 1996

Kaneko, K., Ishii, C., Ruike, M., Kuwabara, H.: Origin of superhigh surface area and microcrystalline graphitic structures of activated carbons. Carbon **30**, 1075–1088 (1992)

Moore, W.J.: Physical Chemistry, 4th edn. Prentice-Hall, New Jersey (1972)

Nitta, T., Shigetomi, T., Kuro-oka, M., Katayama, T.: An adsorption isotherm of multi-site occupancy model for homogeneous surface. J. Chem. Eng. Jpn. **17**, 39–45 (1984)

Shiflett, M.B., Corbin, D.R., Elliott, B.A., Yokozeki, A.: Sorption of trifluoromethane in zeolites and ionic liquid. J. Chem. Thermodyn. **64**, 40–49 (2013a)

Shiflett, M.B., Corbin, D.R., Yokozeki, A.: Comparison of the sorption of trifluoromethane (R-23) on zeolites and in an ionic liquid. J. Ads. Sci. Technol. **31**, 59–84 (2013b)

Shiflett, M.B., Elliott, B.A., Lustig, S.R., Sabesan, S., Kelkar, M.S., Yokozeki, A.: Chemical absorption of carbon dioxide in room-temperature ionic liquid 1-ethyl-3-ethylimidazolium acetate [eeim][Ac]. Chem. Phys. Chem. **13**, 1806–1817 (2012a)

Shiflett, M.B., Junk, C.P., Harmer, M.A., Yokozeki, A.: Solubility and diffusivity of 1,1,1,2-tetrafluoroethane in room-temperature ionic liquids. Fluid Phase Equilib. **242**, 220–232 (2006a)

Shiflett, M.B., Junk, C.P., Harmer, M.A., Yokozeki, A.: Solubility and diffusivity of difluoromethane in room-temperature ionic liquids. J. Chem. Eng. Data **51**, 483–495 (2006b)

Shiflett, M.B., Niehaus, A.M.S., Elliott, B.A., Yokozeki, A.: Phase behavior of N_2O and CO_2 in room-temperature ionic liquids [bmim][Tf_2N], [bmim][BF_4], [bmim][$N(CN)_2$], [bmim][Ac], [eam][NO_3] and [bmim][SCN]. Int. J. Thermophys. **33**, 412–436 (2012b)

Shiflett, M.B., Yokozeki, A.: Binary vapor-liquid and vapor-liquid-liquid equilibria of hydrofluorocarbons (HFC-125 and HFC-143a) and hydrofluoroethers (HFE-125 and HFE-143a) with ionic liquid [emim][Tf_2N]. J. Chem. Eng. Data **53**, 492–497 (2008)

Shiflett, M.B., Yokozeki, A.: Chemical absorption of sulfur dioxide in room-temperature ionic liquids. Ind. Eng. Chem. Res. **49**, 1370–1377 (2010)

Shiflett, M.B., Yokozeki, A.: Gaseous absorption of fluoromethane, fluoroethane, and 1,1,2,2-tetrafluoroethane in 1-butyl-3-methyl-imidazolium hexafluorophosphate. Ind. Chem. Eng. Res. **45**, 6375–6382 (2006a)

Shiflett, M.B., Yokozeki, A.: Hydrogen substitution effect on the solubility of perhalogenated compounds in ionic liquid [bmim][PF_6]. Fluid Phase Equilib. **259**, 210–217 (2007a)

Shiflett, M.B., Yokozeki, A.: Phase behavior of carbon dioxide in ionic liquids: [emim][acetate], [emim][trifluoroacetate], and [emim][acetate] + [emim][trifluoroacetate] mixtures. J. Chem. Eng. Data **54**, 108–114 (2009a)

Shiflett, M.B., Yokozeki, A.: Solubilities and diffusivities of carbon dioxide in ionic liquids: [bmim][PF_6] and [bmim][BF_4]. Ind. Eng. Chem. Res. **44**, 4453–4464 (2005)

Shiflett, M.B., Yokozeki, A.: Solubility and diffusivity of hydrofluorocarbons in room-temperature ionic liquids. AIChE J. **52**, 1205–1219 (2006b)

Shiflett, M.B., Yokozeki, A.: Solubility differences of halocarbon isomers in ionic liquid [emim][Tf_2N]. J. Chem. Eng. Data **52**, 2007–2015 (2007b)

Shiflett, M.B., Yokozeki, A.: Solubility of CO_2 in room-temperature ionic liquid [hmim][Tf_2N]. J. Phys. Chem. B **111**, 2070–2074 (2007c)

Shiflett, M.B., Yokozeki, A.: Solubility of fluorocarbons in room temperature ionic liquids. In: Plechkova, N.V., Rogers, R.D., Seddon, K.R. (eds.) Ionic Liquids: From Knowledge to Applications, ACS Symposium Series 1030, pp. 21–42. American Chemical Society, Washington DC (2009b)

Shiflett, M.B., Yokozeki, A.: Solubility of gases in ionic liquids. In: Plechkova, N.V., Seddon, K.R. (eds.) Ionic Liquids, pp. 349–386. Wiley, UnCOILed (2013)

Shiflett, M.B., Yokozeki, A.: Solubility of N_2O and CO_2 in olive oil. J. Fluid Phase Equilib. **305**, 127–131 (2011)

Surya Prakash, G.K., Jog, P.V., Batamack, P.T.D., Olah, G.A.: Taming of fluoroform: direct nucleophilic trifluoromethylation of Si, B, S, and C Centers. Science **338**, 1324–1327 (2012)

Yang, R.T.: Adsorbents: Fundamentals and Applications, pp. 79–123. Wiley, New Jersey (2003)